Progress In Electromagnetics Research Letters, Vol. 2, 53–61, 2008

FINITE ELEMENT METHOD SIMULATION OF PHOTOINDUCTIVE IMAGING FOR CRACKS

C.-C. Tai and Y.-L. Pan

Department of Electrical Engineering
National Cheng Kung University
Tainan, Taiwan

Abstract—In this paper, the numerical simulations of photoinductive imaging (PI) method have been performed using the finite element method (FEM) with the 2D transient to characterize corner cracks at the edge of a bolt hole. The PI imaging results have higher spatial resolution in the area of the defect in 2D models as compared with the conventional eddy current (EC) images. The FEM simulation results of 0.5-mm rectangular defects are showed and analyzed. The dependencies of PI signals on EC frequencies and temperature of the thermal spot are also examined. The results demonstrate that the PI method is applicable to examine the geometric shape of corner cracks.

1. INTRODUCTION

Crack detection and sizing is a critical issue in quantitative nondestructive evaluation (NDE). The ultrasonic method is used predominantly to detect subsurface discontinuities, while the EC method is effective for surface cracks. However, one of the main disadvantages of conventional eddy current method is the low spatial resolution, which is constrained by the size of eddy current probes. The PI method is a hybrid NDE technique that combines eddy current and laser-based thermal wave methods. The use of a focused laser beam provides the method with a microscopic resolution while using eddy current pickup sensors.

Moulder et al. [1] showed that this new technique dramatically increased image resolutions, and could be used to calibrate and characterize eddy current probes [2–4]. The method experimentally showed the high-resolution capability inherent in this technique by adapting a photoinductive sensor developed for a fiber optic probe to an existing photoacoustic microscope [2]. The same method will work equally well to characterize cracks on thick metals. Determining the crack dimensions is the interesting detection of a corner crack on the surface surrounding a bolt hole, such as depth and length [5].

In this article, we use the finite element method to simulate the photoinductive imaging (PI) technique for bolt-hole cracks inspection. Based on the simulation results, we also discuss the effects of EC frequencies and temperature of the thermal spot, and compare the PI results with EC images for a 0.5-mm triangular notch.

2. THE PHOTOINDUCTIVE IMAGING METHOD

Photoinductive mapping of eddy current fields interacting with cracks is a newly devised technique that is similar to photothermal (PT) imaging. The physical principles underlying it are illustrated in Fig. 1, which shows the coil of an eddy current probe carrying a current placed in close proximity to the specimen surface. A focused laser beam generates a localized hot spot on the specimen surface from above. The temperature fluctuation causes a local change in the electrical conductivity, which in turn induces a change in the impedance of the eddy current probe. The electrical conductivity of specimen is given by the expression:

$$\sigma = \frac{1}{[\rho_0(1 + \alpha(T - T_0))]} \tag{1}$$

where ρ_0 is the resistivity at temperature T_0, and α is the temperature coefficient of the resistivity. T_0 is the temperature 293 K, and T is the actual temperature in the specimen sub-domain.

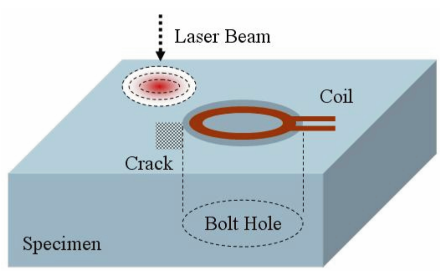

Figure 1. Inspection geometry of the photoinductive field measurement technique.

The PI effect can be calculated as follows. The dependent variable in this application mode is the azimuthal component of the magnetic vector potential, $\mathbf{A}$, which conforms to the following relation:

$$(j\omega\sigma - \omega^2\varepsilon)\mathbf{A} + \nabla \times (\mu^{-1}\nabla \times \mathbf{A}) = \frac{\sigma V_{loop}}{L}, \tag{2}$$

where ω denotes the angular frequency, σ the conductivity, μ the permeability, ε the permittivity, L the length, and V_{loop} the voltage applied to the coil. The conductivity outside the coil is zero. According to the constitutive relation ($C.R.$), the current density ($\mathbf{J}^e$) can be calculated as follows.

$$\mathbf{J}^e = \sigma\mathbf{E} = -\sigma\left(\nabla V + \frac{\partial \mathbf{A}}{\partial t}\right), \tag{3}$$

where $\mathbf{E}$ is the electric field intensity. The electric potential (V) is obtained from Faraday's law. The defining equation for the magnetic vector potential $\mathbf{A}$ is a direct consequence of the magnetic Gauss'law. The induced current (I) in the coil is calculated by the integration of current density in the cross-sectional area (s) of the coil:

$$\int_S \mathbf{J}^e \cdot \mathrm{d}s = I. \tag{4}$$

3. SPECIMEN AND SIMULATION

The specimens used for this study are titanium blocks (Ti-6Al-4V) with 6-mm bolt holes. The notch is 0.5 mm in both length and depth and 0.2 mm in width. The coil probe (inner diameter = 2.54 mm, outer diameter = 4.1 mm, and length = 0.76 mm) was inserted in the bolt hole with the coil firmly positioned flush with the edge of the bolt hole. The actual size geometry of the 2D model for PI imaging method is shown in Fig. 2. The probe was operated at a range of frequencies from 200 kHz to 1 MHz. The temperature produced by laser beam was at a range of from 100°C to 500°C. The simulations were implemented using the COMSOL Multiphysics$^{\text{TM}}$ software. In this work, we use the simplified 2D model for comparing the characteristics of PI imaging method and EC imaging method (Fig. 3). We designed the coil that with a height equal to or greater than the depth of the notch. This is to make sure that the eddy currents surround the whole notch and so that the depth information can be revealed. The distance between the specimen and the coil (diameter = 1 mm, length = 0.76 mm) was 0.1 mm. In the case of EC scan that without the laser point, the coil is moving along the x-axis and cross the notch on specimen. In the PI scan, the coil is fixed right on the center of the notch and the laser is moving in the same direction as the previous case. The uniform scan plan with closely spaced scan lines so that flaw orientation and scan spacing would not affect the outcome was assumed. To calculate the impedance edance ($\Delta Z = V_{loop}/I$) of the coil in the simulations, the total induced eddy current of the coil can be obtained by carrying out sub-domain integration of the total current density for the cross-section of the excited coil.

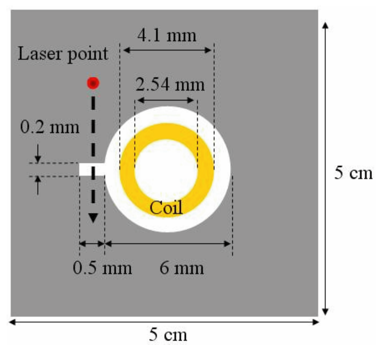

Figure 2. The actual size geometry of the 2D model for PI imaging method. (the bold dotted line is the laser point path).

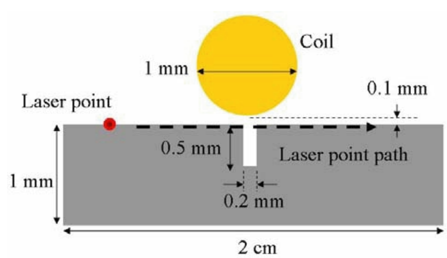

Figure 3. The simplified 2D model for comparing the characteristics of PI imaging method and EC imaging method.

4. RESULTS AND DISCUSSION

The simulation results using the PI imaging method and the conventional EC imaging method are presented and compared in this section. The simulation results of the signals interaction with various temperature and frequency will be first presented. The effects of eddy current were compared by varying the coil excitation frequency from 200 kHz to 1 MHz and the laser beam temperature from 100°C to 500°C. The diffusion of heat from laser beam and the eddy current density distribution around the crack are shown in Fig. 4. The temperature fluctuation causes a local change in the electrical conductivity of the specimen and the current density of the specimen. The lines indicate the contour of induced current density on the coil and the specimen. Figs. 5 and 6 show the signal of coil impedances with EC method and PI method, respectively. The center point of the rectangular notch is 0 mm in x-axis, as shown in Figs. 5 and 6. Fig. 5 is the EC image signals of a 0.5-mm rectangular notch at 600-kHz EC frequency, without laser beam. Fig. 6 is the PI image signals of a 0.5-

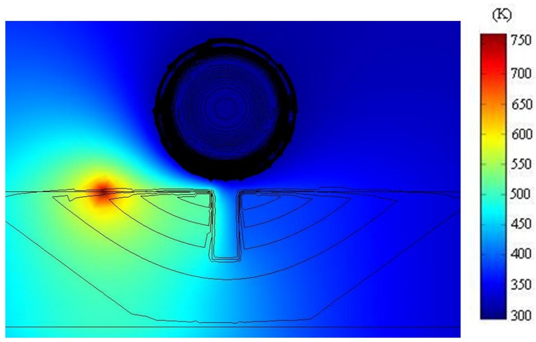

Figure 4. The diffusion of heat from laser beam and eddy current density distributions. EC frequency, 600 kHz; laser temperature, 500°C (773 K).

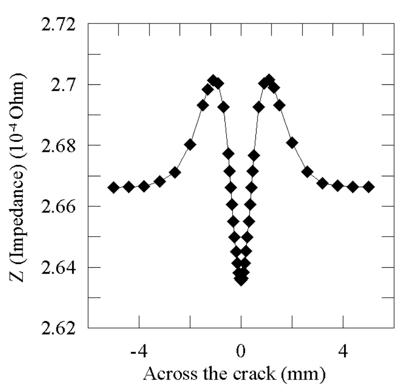

Figure 5. The flaw impedances of EC signal for a 0.5-mm rectangular notch in Ti-6A1-4V. EC frequency, 600 kHz.

mm rectangular notch at the same EC frequency and 300°C laser beam temperature. Because the length of the flaw is less than the diameter of the probe, the flaw scan produces a double-peaked response [6]. As shown in the Figs. 5 and 6, both figures conform to this phenomenon. Comparison of flaw impedance measured with two detection method for rectangular notch, the resolution of PI signal is higher than the EC signal. There is a higher sharp edge in PI signal than in EC signal.

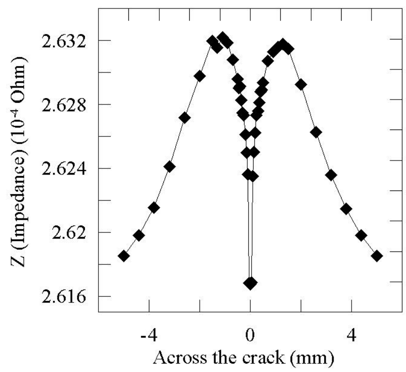

Figure 6. The flaw impedances of PI signal for a 0.5-mm rectangular notch in Ti-6A1-4V. EC frequency, 600 kHz; laser temperature, 300°C.

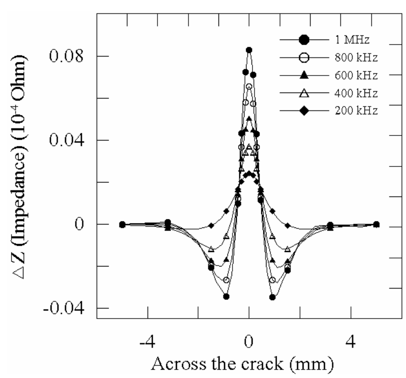

Figure 7. Images with different EC frequency. (EC scan without the laser beam).

The effects of EC frequency on the PI imaging signals and EC imaging signals for transverse scans across a 0.5-mm long and 0.2-mm wide notch are shown in Figs. 7 and 8, respectively. In order to clearly exhibit the crack's effect, the impedance difference between signals with crack and without crack is reported. As shown in Fig. 7, the eddy currents around the crack are more uniform at lower frequencies. But higher EC frequencies generate a stronger PI signal. Fig. 8 illustrates the signal amplitude is increased when higher eddy current frequencies are applied, and therefore the better crack images are obtained by increasing the eddy current frequency. Furthermore, the impedance difference for 200-kHz case is reversed on the notch area. That may due to deeper skin depth and lower current density on the surface of specimens. For the rectangular notches in this titanium alloy, eddy current frequencies above 200 kHz are more suitable for imaging the cracks.

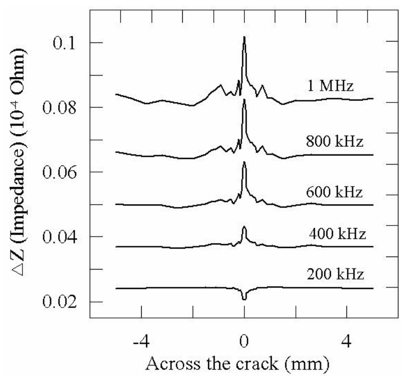

Figure 8. PI imaging signal with different frequency. Laser temperature, 300°C.

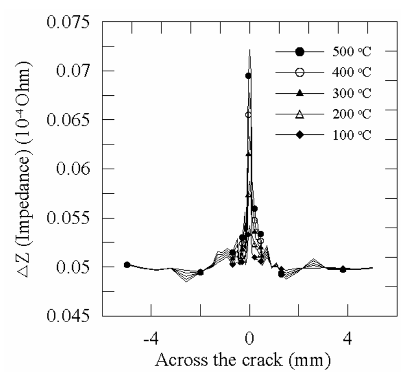

Figure 9. PI imaging signal with different laser point temperature. EC frequency, 600 kHz.

Figure 9 shows that the peak amplitude of PI imaging signals varies with laser point temperature for transverse scans across a 0.5 mm long and 0.2 mm wide notch. There is the same process to clearly display the crack's shape. When lower laser beam temperatures are applied, the peak amplitude of signal is decreased. Because reducing the temperature will generates higher current density and deeper penetration on the surface of this specimen. That makes the eddy currents around the crack are more uniform at lower laser temperature.

5. CONCLUSIONS

The FEM simulation results demonstrate the feasibility of photoinductive imaging method when applied to the detection of corner cracks. The EC frequency and laser beam temperatures affect PI signal amplitude and resolution. The PI images have higher spatial resolution in the area of the defect in 2D models when compared with the conventional EC images. The higher PI signal amplitude can be obtained by increasing the laser beam temperature.

ACKNOWLEDGMENT

This research was supported by the grant from National Science Council, Taiwan (NSC 96-2628-E-006-256-MY3). Also, this work made use of Shared Facilities supported by the Program of Top 100 Universities Advancement, Ministry of Education, Taiwan.

REFERENCES

1. Moulder, J. C., N. Nakagawa, K. S. No, Y. P. Lee, and J. F. McClelland, "Photoinductive imaging: a new NDE technique," *Review of Progress in Quantitative NDE*, D. O. Thompson and D. E. Chimenti (eds.), Vol. 8A, 599, Plenum Press, New York, 1989.
2. Moulder, J. C. and N. Nakagawa, "Characterizing the performance of eddy current probes using photoinductive field-mapping," *Research in Nondestructive Evaluation*, Vol. 4, 221–236, 1992.
3. Hughes, M. S., J. C. Moulder, M. W. Kubovich, and B. A. Auld, "Mapping eddy current probe fields using the photoinductive effect," *NDT & E International*, Vol. 28, 251, 1995.
4. Nakagawa, N. and J. C. Moulder, "Eddy current probe calibration via the photoinductive effect," *NDT and E International*, Vol. 28, 245–246, 1995.

5. Tai, C.-C. and J. C. Moulder, "Bolt-hole corner crack inspection using the photoinductive imaging method," *Journal of Nondestructive Evaluation*, Vol. 19, 81–93, 2000.
6. Auld, B. A., S. R. Jefferies, and J. C. Moulder, "Eddy-current signal analysis and inversion for semielliptical surface cracks," *Journal of Nondestructive Evaluation*, Vol. 7, 79–94, 1988.